A new zero-dimensional dynamic model to study the capacity loss mechanism of vanadium redox flow batteries

Hao Wang[a,*], S. Ali Pourmousavi[a], Yifeng Li[b], Wen L. Soong[a], Xinan Zhang[c], Bingyu Xiong[d]

[a]*School of Electrical & Mechanical Engineering, The University of Adelaide, Australia*
[b]*Voith group, Germany*
[c]*School of Engineering, The University of Western Australia, Australia*
[d]*School of Automation, Wuhan University of Technology, China*

Abstract

The study of the capacity loss mechanisms of vanadium redox flow batteries (VRFBs) is important for optimising battery design and performance. To facilitate this, a new zero-dimensional (0-D) dynamic model is proposed in this study that considers different electrolyte transfer (osmosis and electro-osmosis) and vanadium species crossover (convection, electro-migration and diffusion) mechanisms based on the configuration of a 5 kW/3 kWh VRFB system with cation membranes (Nafion 115). The proposed model is validated under three constant current regimes and achieves a mean absolute error (MAE) of less than 2 %. Furthermore, its accuracy in estimating capacity over 100 cycles is evaluated using the experimental results of a single-cell VRFB system, which achieves a low MAE of 1.9 %. Most importantly, an in-depth analysis of the capacity loss mechanism, including the electrolyte volume transfer, electrolyte imbalance, and electrolyte flow rate, is conducted under different constant current and flow rate regimes. The influence of all electrolyte transfer and crossover mechanisms mentioned above are carefully examined and discussed. This work offers practical recommendations to mitigate capacity loss. Furthermore, the proposed model facilitates the development of electrolyte re-balancing techniques and advanced optimisation methods for optimal battery operation with low computational requirements for battery management systems (BMS).

Keywords: Vanadium redox flow battery, battery modelling, capacity loss, battery management, SOH estimation

*Corresponding Author
Email address: hao.wang05@adelaide.edu.au

1. Introduction

The vanadium redox flow battery (VRFB) has emerged as a reliable and effective large-scale energy storage system (ESS) in various applications of modern power systems. Compared to other mainstream battery technologies, VRFB is more suitable for long-term storage with a low levelised cost of energy (LCOE). This is mainly because its capacity can be restored and it has low apparent capacity degradation [1]. This is achieved using re-balancing devices (i.e., overflow or other electrolyte exchange devices) in the existing commercial VRFB systems [2]. However, it remains crucial to thoroughly understand and analyse the capacity loss mechanism of VRFB for three main reasons:

1. To maximise its capacity utilisation.
2. To develop practical tools for battery design and re-balancing techniques.
3. To develop computationally efficient tools for online capacity and state of health (SOH) estimation.

To fulfil this need, effective battery models are developed by integrating relevant chemical and multi-physics principles to use in battery design studies, optimisation, and mitigating capacity fading of VRFB. However, to the best of our knowledge, there is no systematic study of the capacity loss mechanisms and limitations of large-scale VRFB systems in the literature, which will be explained in detail in the following sections. Most importantly, there is no rigorously validated, computationally efficient and effective 0-D VRFB model that considers various effects of ion transport and electrolyte volume transfer in the literature. Thus, these conventional 0-D models may have relatively low accuracy, which makes them unfit for real-time optimisation, control, electrolyte re-balancing, and other battery management applications. For example, a computationally efficient model is effective for the online estimation of SOH and critical state estimation in battery management systems (BMSs). Previous models that have not been properly validated can have poor performance over long operation cycles, leading to poor battery management and real-time grid-level energy management outcomes that degrade overall battery performance [1].

The existing VRFB models can be divided into two main categories: high- and low-dimensional models. Among the high-dimensional models, two-dimensional (2-D) models are commonly used. Shah et al. proposed the first 2-D transient modelling framework in [3] based on mass, charge, and momentum transport and conservation laws. This work established the foundations for accurate VRFB modelling, which is useful for battery design and model-based studies. Later, Agar et al. developed a 2-D transient model to represent the contribution of ion diffusion, migration, and osmotic and electro-osmotic convention to the crossover of vanadium ions through different membranes [4]. Furthermore, Knehr et al. presented another transient model that considers the transport of water through the membrane to improve the original 2-D transient model [5]. Additionally, Zheng et al. developed a 3-D model in [6] to study the thermal behaviour and temperature distribution of a VRFB unit. Recently, Oh et al. developed a comprehensive 3-D model in [7] to demonstrate electrolyte transfer, vanadium ion crossover, and thermal dynamics in an experimental VRFB system. The simulation results matched well with the experimental data. In addition to the above-mentioned high-dimensional models, several computationally efficient zero-dimensional (0-D) models were developed to simulate VRFB operation for real-time control and optimisation studies. These models offer users with limited knowledge of battery chemistry a simpler way to comprehend the functioning of VRFBs and to simulate them in numerical software (e.g., MATLAB/Simulink and Python) using ordinary differential equations

(ODEs). Tang et al. developed a 0-D VRFB model in [8] that takes into account ion diffusion. Later, Tang et al. extended the model in [9] by incorporating the configuration and energy balance of the VRFB system. Their 0-D VRFB model has been broadly applied in VRFB optimisation and control studies, which demonstrates the underlying benefits of computationally efficient models in these model-based studies. Later, Badrinarayanan et al. proposed another extended dynamic model in [10] to study the effect of temperature on ion diffusion and water transfer. Furthermore, Li et al. developed a new dynamic plug flow reactor model in [11] based on material balance to simulate the distribution imbalance of vanadium species in a cell. Recently, Pugach et al. developed a control-orientated 0-D VRFB cell model that considers all types of vanadium ion crossover mechanisms in [12], which offers a practical tool to study the capacity decay caused by the ion crossover.

One of the main caveats of existing 0-D VRFB models is that they do not incorporate all types of crossover and water transfer mechanisms. Song et al. presented a notable work in [13] that summarised the electrolyte volume change of a VRFB system from three key perspectives: continuous electrolyte transfer from the negative side to the positive side by osmosis, the drag water due to hydrogen ion movement (known as electro-osmosis drag) and water generation/consumption by redox reactions. The water generation/consumption by the redox reaction occurs only on the positive side; thus, it is not responsible for the electrolyte volume transfer that causes the capacity fading. Regarding the crossover of vanadium ions, as indicated by the Nernst–Planck equation, it is mainly driven by diffusion, electromigration, and convection [14]. However, most of the existing 0-D models neglected the influence of electromigration and convection. Moreover, the electrolyte volume transfer by electro-osmosis drag and osmosis has not been considered in most of these models, which is a limiting factor in understanding and modelling the capacity loss mechanism. In addition, these proposed 0-D VRFB models do not adequately include the crossover and electrolyte transfer mechanism, and it can consequentially yield a wrong analysis of the capacity loss mechanism.

Several papers introduced the capacity loss mechanism by crossover and electrolyte volume transfer. Tang et al. [8] discovered that electrolyte imbalance by ion diffusion is one of the main factors that leads to capacity decay, which is determined by the property of the membrane. Later, Badrinarayanan et al. considered the electrolyte transfer mechanism in [10] and found that electrolyte transfer is the main factor that causes long-term capacity decay. Song et al. also found that electrolyte volume transfer is responsible for long-term capacity loss and revealed the relationship between electrolyte flow rate and electrolyte transfer velocity in the laboratory [13]. The electrolyte flow rate is another factor associated with the discharge capacity that has been discussed by Tang et al. [15] and Karrech et al. [16]. They demonstrated that a higher flow rate will provide a sufficient surface concentration level on the electrode to prevent discharge capacity loss. However, these studies analysed the capacity loss factors individually in a non-systematic way and lacked in-depth consideration of all mechanisms. For example, the influence of electrolyte imbalance on electrolyte transfer leading to capacity loss has not been investigated in these studies. In addition, the impact of electro-osmosis drag on the electrolyte volume transfer has been ignored in the existing literature. As a result, conducting a systematic investigation of capacity loss in VRFB systems is necessary to accurately model the factors that contribute to capacity loss. These studies cannot be conducted without developing a new computationally efficient 0-D VRFB model, as the simulation of hundreds of complete charge and discharge cycles would be computationally demanding. In summary, in this work, a new computationally efficient 0-D VRFB model is proposed that involves all crossover and electrolyte transfer mechanisms, which has been rigorously validated for accurate online SOH estimation and in-depth capacity

loss analysis. The capabilities of the model proposed in this paper are compared to those of the existing 0-D models in Table 1.

Table 1: A comparison of crossover and electrolyte transfer mechanisms incorporated in 0-D VRFB models and their validations

	Literature						
Electrolyte transfer mechanism	[8, 9, 15]	[10]	[11]	[12]	[17]	[18]	Proposed
Osmotic	✗	✓	✗	✗	✗	✓	✓
Electro-osmotic	✗	✓	✗	✗	✗	✓	✓
Crossover mechanism							
Diffusion	✓	✓	✓	✓	✓	✓	✓
Electro-migration	✗	✗	✗	✓	✓	✗	✓
Convection	✗	✗	✗	✗	✓	✗	✓
Model validations							
Voltage	✗	✗	✗	✓	✓	✓	✓
Capacity & SOH	✗	✓	✗	✗	✗	✗	✓

The main contributions of this paper are listed below.

- A new 0-D model is developed that considers diffusion, convection, and electro-migration of vanadium species together with the electrolyte transfer mechanism through osmosis and electro-osmosis.
- The proposed model is validated by experimental data from a 5 kW/3 kWh VRFB system under three constant current regimes and experimental data from a single-cell VRFB system for 100 cycles, where it achieved approximately 1.9% mean absolute error (MAE) in the estimation of SOH.
- The vanadium species crossover and electrolyte transfer mechanism are fully investigated and explained in detail.
- In-depth analysis is conducted to study the capacity loss of the 5 kW/3 kWh VRFBs due to crossover and electrolyte volume transfer over 500 cycles, and important conclusions are made to summarise the capacity loss mechanism following the previous studies.

This paper is organised as follows: Section 2 introduces the new proposed 0-D model of a VRFB system. Then extensive simulation studies are carried out to validate the proposed 0-D model and the results are given in Section 3. Moreover, additional simulation results are presented in this section to analyse the capacity loss mechanism of the 5 kW/3 kWh VRFB system in-depth. The influence of electrolyte transfer and ion crossover mechanisms is considered, and their contributions are shown. Finally, the conclusion and future work are given in Section 4.

2. Methods for model development

To study crossover and electrolyte transfer mechanisms for a VRFB system, a new dynamic 0-D multi-physics VRFB model that considers the vanadium ion crossover by diffusion, electro-migration and convection, along with the electrolyte volume transfer mechanisms by osmosis and electro-osmosis is developed in this study. As the dominant flow battery technology, a VRFB system is normally composed of two electrolyte storage tanks, a stack, two pumps, and pipes, as

illustrated in Fig. 1. Two pumps are connected in the battery system for electrolyte circulation to supply active vanadium species during charging/discharging operation. The main chemical reactions in positive/negative half cells and the overall cell reaction are:

Negative half cell reaction:

$$V^{3+} + e^{-} \underset{\text{Discharge}}{\overset{\text{Charge}}{\rightleftharpoons}} V^{2+} \quad E_N^0 = -0.255\text{V} \tag{1}$$

Positive half cell reaction:

$$VO^{2+} + H_2O \underset{\text{Discharge}}{\overset{\text{Charge}}{\rightleftharpoons}} VO_2^{+} + 2H^{+} + e^{-} \quad E_P^0 = 1.004\text{V} \tag{2}$$

Overall cell reaction:

$$VO^{2+} + V^{3+} + H_2O \underset{\text{Discharge}}{\overset{\text{Charge}}{\rightleftharpoons}} VO_2^{+} + V^{2+} + 2H^{+} \tag{3}$$

Note that E_N^0 and E_P^0 are the negative and positive half cell potentials.

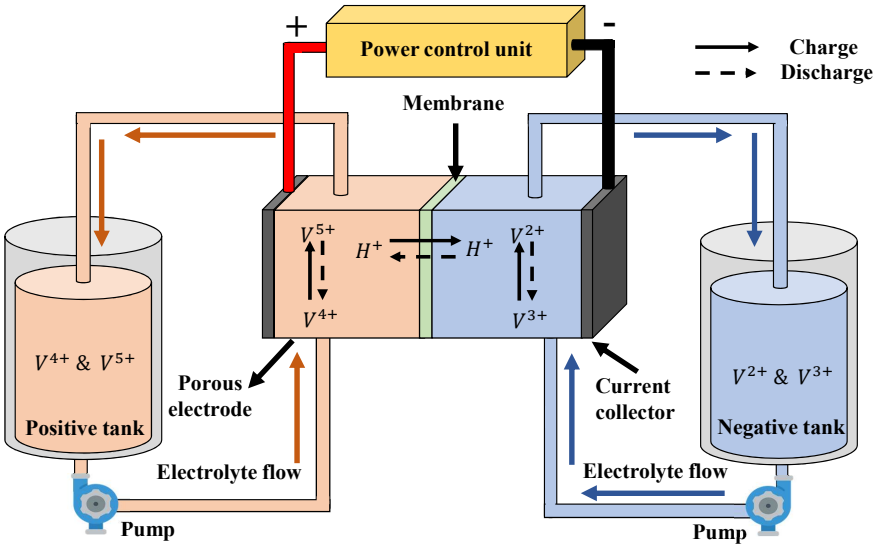

Figure 1: A schematic of a typical VRFB system showing its components and structure

The basic assumptions for this model are:

- The evolution of hydrogen and oxygen gases can be minimised by a good battery design and adequate cutoff voltage (1.1-1.7 V for the single cell), SOC limits (15- 85%) and electrolyte flow rate [19]. Thus, the effect of gas evolution and related side reactions are not considered in this study.
- The temperature distribution in the VRFB system is uniform and assumed constant and equal to the room temperature (25°C).

- Vanadium ions are uniformly distributed in the electrolyte storage tanks and stack [19, 20, 21].
- The overall resistance of the stack remains constant [20].
- The effect of the shunt current is minor and can be ignored [19, 20, 21].
- The volume difference between the negative and positive tanks is caused by electrolyte transfer [20].

2.1. Electrolyte volume transfer model

The ongoing electrolyte volume transfer between the half cells during battery operation plays a critical role in the loss of capacity of VRFBs. The electrolyte volume transfer rate is significant for VRFB systems with cation membranes due to the ionic potential and the osmotic pressure, as indicated by experimental validations [19]. The mechanism of electrolyte volume change is explained in three aspects [13], as shown in Fig. 2 (a).

1. Water consumption and generation in the positive half cell by redox reactions.
2. Transfer of dragged water across the membrane due to the movement of hydrogen ions, which is also known as electro-osmotic drag [22].
3. Osmotic pressure difference between the negative and positive sides, also known as electrolyte osmosis.

As explained by Song et al. in [13], the first two aspects lead to minor variations in the volume of the electrolyte on the positive and negative sides over many operation cycles. Theoretically, they do not have an accumulated effect on the electrolyte volume with the increase of charging/discharging cycles. Furthermore, water consumption and generation in the positive half cells will not cause the transfer of electrolytes across the membrane. It is concluded in [13] that osmosis is the main reason behind continuous electrolyte transfer from the negative side to the positive side of the VRFB system, thus degrading battery capacity [10]. For example, Badrinarayanan et al. [10] formulated an electrolyte volume transfer model that considering the convection of electrolyte transfer from the positive half cell to the negative half cell. However, recent studies by Yang et al. [23] and Lei et al. [24] indicate that the effect of the electric field cannot be ignored, which will affect the electrolyte transport across the membrane. As a result, the electrolyte transfer mechanism considered in this study is mainly driven by the electric field due to ionic potentials and osmotic pressure, which are named electro-osmosis and osmosis. It is notable in this study that redox reactions for water generation and consumption in the half cell are neglected because they have almost no impact on the electrolyte volume transfer between half cells [13]. Thus, their impacts are limited in battery capacity degradation over long operational cycles.

2.1.1. Electrolyte volume transfer by osmosis

Recent studies by Song et al. [13] and Shin et al. [25] have shown that electrolyte osmosis can be mitigated by using different electrolyte flow rates on half cells and adopting different initial electrolyte concentration levels in the anode and cathode. Essentially, these two methods reduce the electrolyte transfer by reducing the osmotic pressure difference across the membrane, and both are associated with the viscosity difference between the anolyte and the catholyte. To model electrolyte transfer from the negative half cells to the positive half cells by osmosis, Darcy's law

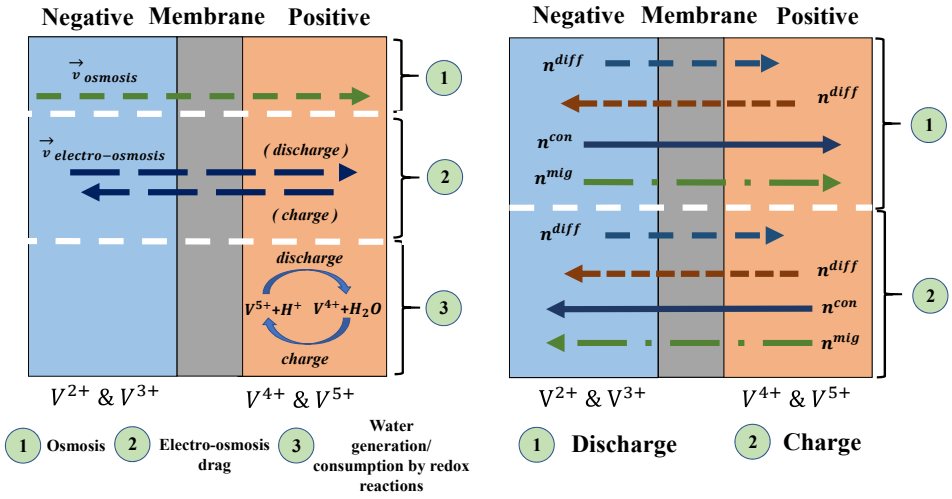

(a) Water transfer mechanism

(b) Crossover mechanism

Figure 2: Electrolyte transfer and crossover mechanisms inside a single VRFB cell

is adopted that describes the dynamic movement of fluid (negative electrolyte) through the porous medium (membrane) from negative half cells to positive half cells:

$$\vec{v}_{osmosis} = \frac{\kappa_m}{\mu^- D}(P^- - P^+) \tag{4}$$

where $\vec{v}_{osmosis}$ is the electrolyte viscosity across the membrane by osmosis, κ_m, A_m, and D are the membrane hydraulic permeability, area, and thickness, respectively. Moreover, μ^- is the electrolyte viscosity on the negative side. P^- and P^+ are the pressure at negative and positive half cells, respectively, which can be calculated by:

$$\begin{aligned} P^- &= \frac{\mu^- \cdot L_e \cdot Q_c}{2 \cdot \kappa_e \cdot A_e} \\ P^+ &= \frac{\mu^+ \cdot L_e \cdot Q_c}{2 \cdot \kappa_e \cdot A_e} \end{aligned} \tag{5}$$

Note that Q_c is the cell electrolyte flow rate and L_e is the length of the electrode, μ^- and μ^+ are the electrolyte viscosity in the negative and positive half cells, respectively, κ_e is the electrode permeability and A_e is the cross sectional area of the electrode through which the electrolyte flows. Combining Eqs. (4)-(5), the electrolyte viscosity by osmosis can be expressed as [13]:

$$\vec{v}_{osmosis} = \frac{\kappa_m}{D} \cdot \frac{L_e}{2\kappa_e A_e} \cdot \left(Q_c - \frac{\mu^+}{\mu^-} Q_c \right) \tag{6}$$

The permeability of the electrode can be derived from [15]:

$$\kappa_e = \frac{d_f^2}{16\lambda_{KC}} \frac{\varepsilon^3}{(1-\varepsilon)^2} \tag{7}$$

where d_f is the fibre diameter of the electrode, ε is the electrode porosity, and λ_{KC} is the Kozenye-Carman constant.

The experimental results in [13] indicate that the viscosity of the electrolyte in the positive and negative half cells varies with the SOC and the total concentration level of the vanadium species. The dynamic viscosity ratio $\frac{\mu^+}{\mu^-}$ (1.5M electrolyte) used in this study is obtained from the experimental results reported in [13].

2.1.2. Electrolyte volume transfer by electro-osmosis

The velocity within the membrane is jointly driven by the osmotic pressure and the ionic potential gradients. Electrolyte movement due to the ionic potential generally refers to electro-osmotic drag [22]. Here, Schlogl's equation is adopted to model the convective transport of the bulk electrolyte by electro-osmosis [26], which is described by:

$$\vec{v}_{electro-osmosis} = -\frac{\kappa_\varphi}{\mu_w} c_f F \left(\nabla\phi^m + \phi^m_{diff}\right) \tag{8}$$

where κ_φ is the electro-kinetic permeability of the membrane and μ_w is the mean viscosity of the electrolyte, and c_f is the fixed acid concentration . $\nabla\phi^m$ is the ionic potential drop, which can be derived based on Ohm's law [27]:

$$\nabla\phi^m = \phi^m_{neg} - \phi^m_{pos} = \frac{I}{\sigma_m A_m} \tag{9}$$

In this equation, σ_m is the effective conductivity of the membrane, where its original and simplified derivations can be obtained using the Nernst-Einstein equation [17, 28], as follows:

$$\sigma_m = \frac{F^2}{RT}\sum_i z_i^2 c_i k_i \approx \frac{F^2}{RT} c_{H^+} k_{\mathrm{H}^+} \tag{10}$$

Note that c_i, k_i, and z_i are the concentration, diffusion coefficients, and valency of different ions. The term ϕ^m_{diff} in Eq. (8) is the effective diffusion potential, which can be calculated by the contribution of each vanadium ion species as [29]:

$$\phi^m_{diff} = \frac{F\sum z_i k_i^m \nabla c_i^m}{\sigma_m} \tag{11}$$

Therefore, the velocity of the electrolyte across the membrane can be formulated as follows:

$$\vec{v}_m = \vec{v}_{electro-osmosis} + \vec{v}_{osmosis} \tag{12}$$

Finally, the electrolyte volume transfer rate from the negative half cells to the positive half cells can be represented by the following equations:

$$\Delta V_N = \vec{v}_m\, A_m \tag{13}$$

$$\Delta V_P = -\,\vec{v}_m\, A_m \tag{14}$$

2.2. Mass balance model

Lutz et al. [30] reviewed several vanadium species transport models from the literature and summarised that diffusion is the most significant factor responsible for vanadium ion crossover. The Nernst-Planck equation indicates that the vanadium ion crossover through the porous medium is mainly due to the force driven by diffusion, electro-migration, and convection [12, 4, 26, 23]. The simulation results obtained from the proposed transient 2-D model in [23] showed that electro-migration and convection are not as significant as diffusion in the crossover flux of vanadium species. However, it still tends to reduce the overall crossover flux by ion diffusion during the charging period and to increase the crossover flux during the discharging period. The crossover mechanism inside a single cell is shown in Fig. 2 (b). During discharging, the net transport of vanadium species by migration and convection has the same direction and becomes opposite during the charging process, as indicated in [23].

Note that the diffusion of vanadium ion species is driven by the concentration gradient across the membrane, and the electro-migration of the vanadium ion species is driven by the ionic potential. Convection is jointly driven by the pressure gradient and the ionic potential as a result of the electrolyte velocity within the membrane. By applying the Nernst-Planck equation, diffusion flux, convection flux, and electro-migration flux can be derived as follows, respectively:

$$n_i^{diff} = k_i \frac{c_i}{D} \tag{15}$$

$$n_i^{con} = \vec{v}_m \tag{16}$$

$$n_i^{mig} = \frac{z_i F}{RT} k_i c_i \nabla(\phi_{neg}^m - \phi_{pos}^m) \tag{17}$$

The overall crossover flux by diffusion, electro-migration, and convection for different vanadium species is given as:

$$n_i^{cross} = n_i^{diff} + n_i^{con} + n_i^{mig} \tag{18}$$

The mass balance equations are adopted from [9] to simulate vanadium ion transport across the membrane. Additionally, considering the hydraulic circulation within the VRFB system, the impact of the flow rate on the ion transport from the electrolyte storage tanks to the cells is modelled. As a result, the variation of the four oxidation states of vanadium ions in the stack and electrolyte storage tanks can be modelled based on the mass balance equations separately, as shown in Eqs. (19)-(26). The definition and numerical value of each parameter are given in Table 2, which are obtained from an experimental 5 kW/3 kWh VRFB system reported in [31].

For vanadium ions in the cell:

$$\frac{dc_2^s}{dt} = \frac{Q_c\left(c_2^t - c_2^s\right) \pm \frac{I}{zF} - n_2^{cross} A_m - 2n_5^{cross} A_m - n_4^{cross} A_m}{L_e W_e H_e} \tag{19}$$

$$\frac{dc_3^s}{dt} = \frac{Q_c\left(c_3^t - c_3^s\right) \mp \frac{I}{zF} - n_3^{cross} A_m + 3n_5^{cross} A_m + 2n_4^{cross} A_m}{L_e W_e H_e} \tag{20}$$

$$\frac{dc_4^s}{dt} = \frac{Q_c\left(c_4^t - c_4^s\right) \mp \frac{I}{zF} - n_2^{cross} A_m + 3n_2^{cross} A_m + 2n_3^{cross} A_m}{L_e W_e H_e} \tag{21}$$

$$\frac{dc_5^s}{dt} = \frac{Q_c\left(c_5^t - c_5^s\right) \pm \frac{I}{zF} - n_5^{cross}A_m - 2n_2^{cross}A_m - n_3^{cross}A_m}{L_e W_e H_e} \tag{22}$$

For vanadium ions in the tanks:

$$(V_N + N\,\Delta V_N)\frac{dc_2^t}{dt} = Q_{system}\left(c_2^s - c_2^t\right) \tag{23}$$

$$(V_N + N\,\Delta V_N)\frac{dc_3^t}{dt} = Q_{system}\left(c_3^s - c_3^t\right) \tag{24}$$

$$(V_P + N\,\Delta V_P)\frac{dc_4^t}{dt} = Q_{system}\left(c_4^s - c_4^t\right) \tag{25}$$

$$(V_P + N\,\Delta V_P)\frac{dc_5^t}{dt} = Q_{system}\left(c_5^s - c_5^t\right) \tag{26}$$

Note that in Eqs. (23)-(26), the electrolyte transfer mechanism is taken into account in our proposed dynamic model, where ΔV_P and ΔV_N are the rates of electrolyte transfer.

2.3. Multi-physics model

In this section, the multi-physics model is formulated to link the chemical characteristics with the electrical parameters. The derivation of the open circuit voltage (OCV) for a single VRFB cell can be formulated as in [18]:

$$E^{OCV} = E^{0'} + \frac{RT}{zF}\ln\left(\frac{c_2^s c_5^s}{c_3^s c_4^s}\right);\ E^{0'} = 1.40\ V \tag{27}$$

The concentration overpotentials, as an important part of overpotentials, can be derived by the following equations in the charging/discharging processes independently:

$$\eta_{con}^{+} = \begin{cases} -\frac{RT}{zF}\ln\left(1 - \frac{I}{nFk_m L_e H_e c_4^s}\right), & \text{charging} \\ -\frac{RT}{zF}\ln\left(1 - \frac{I}{nFk_m L_e H_e c_5^s}\right), & \text{discharging} \end{cases} \tag{28}$$

$$\eta_{con}^{-} = \begin{cases} -\frac{RT}{zF}\ln\left(1 - \frac{I}{nFk_m L_e H_e c_3^s}\right), & \text{charging} \\ -\frac{RT}{zF}\ln\left(1 - \frac{I}{nFk_m L_e H_e c_2^s}\right), & \text{discharging} \end{cases} \tag{29}$$

where k_m is the mass transfer coefficient in dm s^{-1}, which can be derived by [18]:

$$k_m = 1.6 \times 10^{-3}\left(\frac{Q_c}{10 L_e W_e}\right)^{0.4} \tag{30}$$

The activation overpotentials (η_a^+ and η_a^-) are relatively small compared to the ohmic and concentration overpotentials. Normally, activation overpotentials can be combined with the cell ohmic overpotential (Ir) to form the overall cell ohmic overpotential (Ir') [18], where its derivation is as follows:

Table 2: VRFB model parameters and their definitions adopted in this study

Symbol	Definition	Value
N	Number of cells in the stack	37
c	Total concentration of vanadium ions in mol L^{-1}	1.5
V_N	Volume of the electrolyte in negative tank in L	70
V_P	Volume of the electrolyte in positive tank in L	70
H_e	Height of the electrode in m	0.3
L_e	Length of the electrode in m	0.7
W_e	Width of the electrode in m	2.5×10^{-3}
A_m	Membrane area in m^2	0.21
D	Thickness of the membrane in m	1.27×10^{-4} [32]
T	Ambient temperature in K	298.15
R	Gas constant in J mol^{-1} K^{-1}	8.314 [32]
ρ	Electrolyte density in kg m^{-3}	1300 [32]
F	Faraday's constant in C mol^{-1}	96,485 [32]
r'	Overall cell resistance in Ω	1.3×10^{-3}
k_2	Diffusion coefficient of V^{2+} in m^2s^{-1}	8.768×10^{-12} [32]
k_3	Diffusion coefficient of V^{3+} in m^2s^{-1}	3.222×10^{-12} [32]
k_4	Diffusion coefficient of V^{4+} in m^2s^{-1}	6.825×10^{-12} [32]
k_5	Diffusion coefficient of V^{5+} in m^2s^{-1}	5.897×10^{-12} [32]
k_{H^+}	Diffusion coefficient of H^+ in m^2s^{-1}	3.35×10^{-9} [7]
A	Cross sectional area of the porous electrode in m^2	7×10^{-4}
d_f	Fibre diameter of the channel in m	1.76×10^{-5} [32]
ε	Electrode porosity	0.93
λ_{KC}	Kozenye-Carman constant	4.28 [32]
κ_m	Membrane hydraulic permeability in m^2	5×10^{-20}[33]
κ_φ	Membrane electro-kinetic permeability in m^2	1.13×10^{-20} [10]
μ_w	Mean viscosity of bulk electrolyte in Pa s	4.2×10^{-3}[13]
c_f	Fixed acid concentration in mol L^{-1}	2.5

$$Ir' = Ir + \eta_a^+ + \eta_a^- \tag{31}$$

The total stack voltage can then be represented as the sum of the OCV and the overpotentials [18]:

$$E_{\text{stack}} = N(E^{OCV} + ir' + \eta_{con}^+ + \eta_{con}^-) \tag{32}$$

The SOC and SOH are estimated using the following equations, which consider the system imbalance [12]:

$$SOC = \min\left(\frac{c_2^t}{c_2^t + c_3^t}, \frac{c_5^t}{c_4^t + c_5^t}\right) \tag{33}$$

$$SOH = \frac{E_{discharge}}{E_{max}} \tag{34}$$

The E_{max} is the maximum discharge capacity of the battery. Note that the parameters definitions used in the proposed model are given in Table 2 with their values.

3. Simulation results

In this section, simulation studies are conducted using the proposed dynamic 0-D model to investigate the capacity loss mechanism based on the 5 kW/3 kWh VRFB system and the

experimental data of a single cell VRFB system from Pacific Northwest National Laboratory (PNNL) [34].

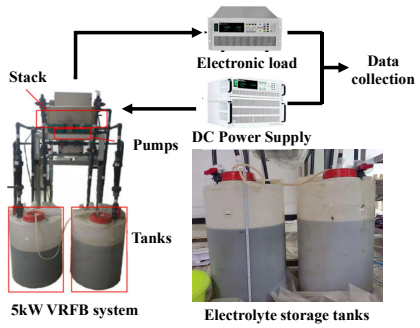

(a) Schematic of the 5 kW/3 kWh experimental VRFB system

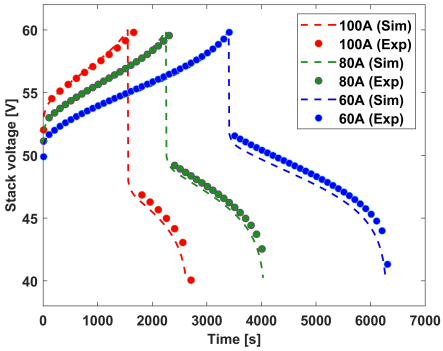

(b) Stack voltage estimation of the 5kW/3kWh VRFB system (under 60A, 80A and 100A constant currents)

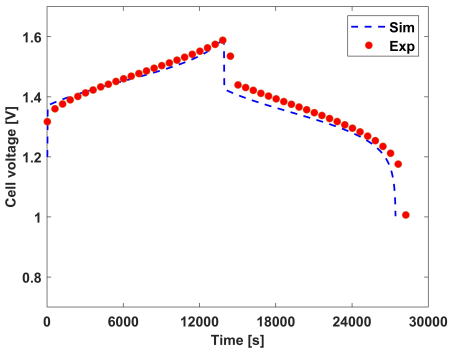

(c) Cell voltage estimation of the single cell VRFB system (first cycle of 0.5A charge/discharge currents)

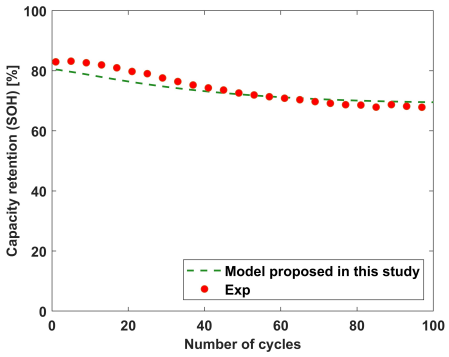

(d) Capacity degradation estimation of the single cell VRFB system over 100 complete cycles

Figure 3: Schematic of the 5 kW/3 kWh experimental VRFB system and model validation results under three different current regimes of the 5kW/3kWh VRFB system and the model validation results of a single cell VRFB system by the proposed 0-D model

3.1. Model performance

An experimental 5 kW/3 kWh VRFB system was set up in a room temperature environment of around 25 °C, as reported in [31]. The upper and lower cutoff voltage limits, minimum concentration level of vanadium ion species for the four oxidation states, the operating current range, and the SOC limits are set as operational constraints in the simulation studies, the values of which are given in Table 3. The membrane of this 5 kW/3 kWh VRFB system is Nafion 115, and the diffusion coefficient is considered constant, which neglects the minor temperature variations in the system. The electrolyte flow rate is set by the pumps on the negative and positive sides, and the transport delay of the electrolytes is neglected.

Table 3: Cutoff limits and other operational constraints adopted for simulation of a 5 kW/3 kWh VRFB system

Simulation constraints and conditions	Range
Cutoff voltage range	40.7-62.9 V
Operational SOC range	0.15-0.85
Operational current range	40-100 A
Flow rate range	0.1-1.2 L/s
Minimum vanadium species concentration level	0.2 mol L^{-1}
Initial SOC	0.15 mol L^{-1}
Operating temperature	25 ^{o}C

The stack in this VRFB system is composed of 37 cells, with dimensions of 750 mm × 480 mm × 350 mm. The two electrolyte storage tanks are of the same size with a radius of 225 mm, and the electrolyte heights in both tanks are about 43 cm from Fig. 3 (a). The average electrolyte storage in the two tanks is about 70 L, and it is assumed that the system is fully balanced. The operating cutoff voltage limits are 40-60 V, and a constant pump speed of 1 m^3/h is used to evaluate the performance of the model. A DC power supply and electronic load are used to charge and discharge the battery, which is controlled in the LabVIEW environment, and the experimental data were transmitted and collected by the host computer, as indicated in Fig. 3 (a). The proposed 0-D model is validated and the results are shown in Fig. 3 (b) under a constant current of 60 A, 80 A, and 100 A. The maximum error in these three cases is less than 1 V, with a mean average error (MAE) of less than 2%, which shows a good estimation using the proposed model. However, due to the lack of experimental data on battery capacity over several cycles with a system that is initially balanced, the efficacy of the proposed model in estimating the capacity over the number of cycles remains unverified. To further validate the performance of the proposed model, a set of single cell experimental data from PNNL is adopted [34]. The configurations of the electrode, electrolyte, and membrane (Nafion 115) are given in the document and are listed in Table 4. As the same membrane is used in this study, the diffusion coefficients of the vanadium species and the hydraulic and electro-kinetic permeabilities remain the same, as shown in Table 2. Note that other unknown noncritical parameters are simply kept the same, as shown in Table 2. The cutoff voltage limit is 0.8-1.6 V, where the experiments are carried out using 0.5 A charge/discharge current under 100 complete cycles with a constant flow rate of 20 ml/min. The temperature is assumed to be 25 ^{o}C.

Table 4: VRFB model parameters and their definition for the single-cell VRFB system from [34]

Symbol	Definition	Value
c	Total concentration of vanadium ions in mol L^{-1}	2
V_N	Volume of the electrolyte in negative tank in L	5×10^{-2}
V_P	Volume of the electrolyte in positive tank in L	5×10^{-2}
H_e	Height of the electrode in m	5×10^{-2}
L_e	Length of the electrode in m	2×10^{-2}
W_e	Width of the electrode in m	3.7×10^{-3}
A_m	Membrane area in m^2	1×10^{-3}
D	Thickness of the membrane in m	1.27×10^{-4}
r'	Overall cell resistance in Ω	0.1
ε	Electrode porosity	0.67
c_f	Fixed acid concentration in mol L^{-1}	3.5

In Fig. 3 (c) and (d), the performance of the proposed model is shown compared to the experimental results of a single cell VRFB system. From Fig. 3 (c), it can be seen that the proposed model achieves high accuracy with an MAE of less than 2%. Most importantly, the results in Fig. 3 (d) demonstrate the accuracy of the proposed 0-D model in accurately estimating capacity degradation with an MAE of 1.9%, which is comparable to the results reported in previous work by Yang et al. (less than 3%) in [23] and Knehr et al. (4.2%) in [5] using 2-D transient models. Note that the 100% capacity defined in this figure is the maximum capacity achieved from the low current discharge test of the single cell VRFB system by PNNL, which is approximately 2.33 Ah. To the best of our knowledge, this is the first rigorous validation of the 0-D transient model for the estimation of capacity degradation based on long-term experimental data, 100 complete charge and discharge cycles in this case. Compared to 2-D and 1-D models, our proposed 0-D model has extremely low computational complexity (eliminating the need for finite element modelling) and holds great potential for application in BMS to accurately estimate the battery's SOH. In particular, the proposed 0-D model takes 6 s to simulate 287,500 time steps using a desktop machine with an Intel® Core™ i7-10700 CPU (2.90 GHz), which has a speed of around 2.1 μs per step.

The rest of the paper will be devoted to analysing the capacity loss in a 5 kW/3 kWh industrial-scale VRFB system using the proposed 0-D model and providing a detailed analysis of the results.

3.2. The capacity loss from the electrolyte volume transfer

The flow rate of the electrolyte is proportional to the pressure difference across the membrane as mentioned in Section 2.1 and as indicated in Eq. (4), thus influencing the rate of electrolyte osmosis from the positive side to the negative side. In previous studies, such as the modelling works by Badrinarayanan et al. [10] and Jirabovornwisut et al. [35], electrolyte volume transfer is identified as one of the factors that cause long-term capacity loss for VRFBs, and this is supported by experimental validation in [13]. Therefore, the electrolyte flow rate is one of the main factors causing capacity loss, and therefore its impact must be examined by simulation studies.

To investigate the impact of electrolyte flow rate on volume transfer and capacity change, a simulation study is carried out using the model designed for the 5 kW/3 kWh VRFB system. The charging and discharge currents adopted in this study are 100 A. The cutoff limits and other operational constraints in this study are the same as in Table 3. In Fig. 4, the capacity variations and the amount of transfer of the electrolyte volume are given using constant flow rates of 0.4, 0.8, and 1.2 L/s for 500 cycles. It is important to note that this study strategically employed an electrolyte flow rate that exceeds the operational norms of typical VRFB setups. This choice aims to accentuate the pace of electrolyte migration driven by osmosis, enabling a more comprehensive analysis of the capacity variations arising from electrolyte transfer phenomena. It is evident from Fig. 4 (b) that a higher flow rate causes a faster transfer rate of the electrolyte volume due to the increase in the osmotic pressure across the membrane. Consequently, a more rapid capacity reduction is observed with a flow rate of 1.2 L/s, as illustrated in Fig. 4 (a), particularly after 250 cycles. Continuous electrolyte transfer from the negative side to the positive side causes the loss of V^{2+} and V^{3+} species. This process is accelerated with the increase of the electrolyte flow rate, which increases the electrolyte transfer rate according to Darcy's law, expanding the electrolyte imbalance in the VRFB system. An additional proof will be presented later to support the explanation. As a result, this decreases the capacity of the VRFB system over long operational cycles and accumulates with an increasing number of cycles. The results using

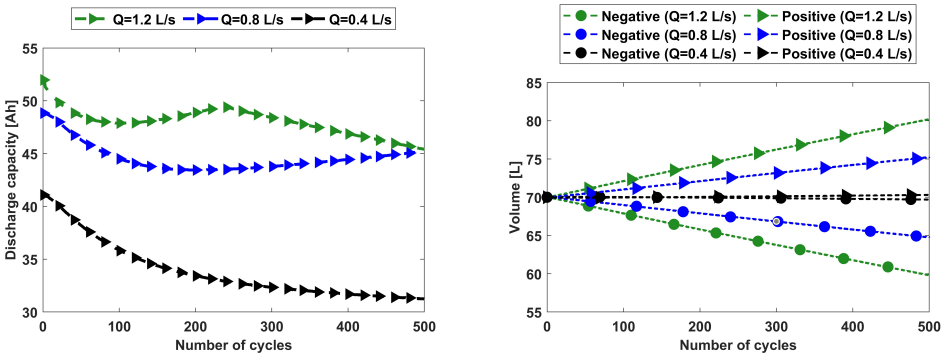

(a) Capacity profiles vs. electrolyte flow rate over 500 cycles

(b) Electrolyte volume profiles vs. electrolyte flow rate over 500 cycles

Figure 4: Capacity and electrolyte volume profiles of different constant flow rates with 100 A operational currents over 500 cycles

a flow rate of 0.8 L/s show an initial reduction in capacity followed by a recovery after 200 cycles without a continuous reduction over the entire 500 cycles. This can be attributed to the crossover of vanadium species that results in electrolyte imbalance, and a detailed explanation will be presented in the next section. Furthermore, the discharge capacity at a flow rate of 0.4 L/s exhibits a lower capacity over 500 cycles. This can be attributed to the electrolyte flow rate having an influence on the overpotential and thus affecting the depth of discharge (DOD). The influence of the electrolyte flow rate on the discharge capacity will be further investigated in this section. Furthermore, this discharge capacity with a flow rate of 0.4 L/s exhibits rapid reduction before reaching 200 cycles, although there is no significant transfer of the electrolyte volume. Indeed, this is caused by the difference in vanadium ion crossover rate by convection that has an impact on the electrolyte concentration. More results will be provided on the electrolyte concentration difference in Section 3.3 for a thorough examination.

From the illustration in Fig. 2 (a), it can be seen that the electrolyte transfer across the membrane is mainly governed by the osmosis and the electro-osmosis drag, which are driven by the osmotic pressure and the electric field in the electrolyte, respectively. In Fig. 5, the electrolyte transfer rate by osmosis and electro-osmosis over a complete charge and discharge cycle and net electrolyte crossover are shown for 500 cycles. Note that the positive values of the electrolyte volume transfer rate in Fig. 5 indicate the transfer of the electrolyte from the negative side to the positive side, and vice versa. The rates of electrolyte volume transfer by osmosis under different flow rates are given in Fig. 5 (a), where it can be seen that the osmotic pressure is proportional to the electrolyte flow rate and is associated with viscosity, as indicated in Eq. 6. The osmosis leads to a continuous transfer of the electrolyte volume from the negative side to the positive side. However, the electro-osmosis drag is another driving force due to the electric field across the membrane, where it is bi-directional in the charging/discharging processes, as the results demonstrate in Fig. 5 (b).

Song et al. explained that the net transfer of electrolytes by electro-osmosis drag is approximately zero in a full charge and discharge cycle in [13]. However, the underlying assumption is that the charge time is equal to the discharge time, which is unlikely to happen considering the

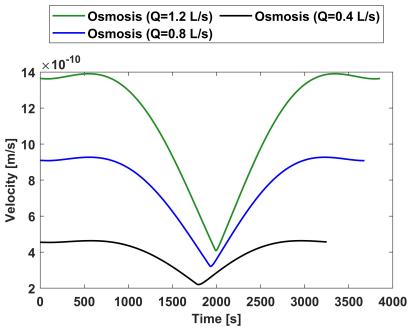

(a) Electrolyte volume transfer rate by osmosis vs. time for different electrolyte flow rates at 100 A

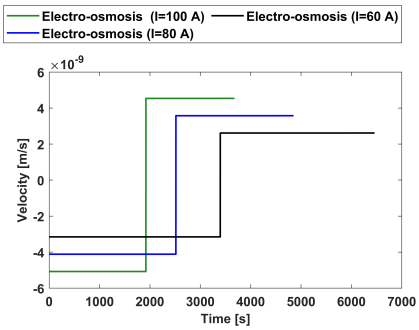

(b) Electrolyte volume transfer rate by electro-osmosis drag vs. time for different currents with 0.8 L/s flow rate

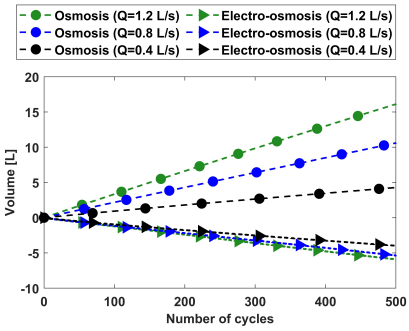

(c) Net transferred volume by osmosis and electro-osmosis over 500 cycles

Figure 5: Velocity profiles of osmosis and electro-osmosis for one full charge and discharge cycle and their net volume transfer over 500 cycles

long-term battery operation. Moreover, a study related to electrolyte volume transfer by Oh et al. showed that electrolyte volume transfer by electro-osmosis drag cannot be net zero during a full charge and discharge cycle [7]. As a result of the difference in charge and discharge time, the electrolyte volume transfer by electro-osmosis tends to accumulate over long operational cycles, and its influence has to be considered. More results are provided in Fig. 5 (c) to investigate the contribution of osmosis and electro-osmosis in long-term electrolyte transfer. It can be seen that the electrolyte transfer by electro-osmosis is accumulated as a result of the charge and discharge time difference and tends to reduce the net electrolyte transfer from the negative side to the positive side. Moreover, the electrolyte volume transfer by electro-osmosis accumulates with increasing operational cycles. However, osmosis is more significant for electrolyte volume transfer in comparison with electro-osmosis, which causes persistent electrolyte transfer during the operational period. This proves that electro-osmosis has a non-negligible impact on the electrolyte volume transfer over long-term operation. However, electrolyte volume transfer by electro-osmosis has been neglected in the previous literature because of the neglect of the long-term operation of VRFBs.

3.3. The capacity loss from the vanadium species crossover

Tang et al. [8] developed a dynamic 0-D model that considers the crossover by ion diffusion to study the capacity loss of a VRFB system. Their model is proposed to study the long-term capacity loss caused by ion diffusion, also known as the electrolyte concentration imbalance. However, in their study, the electrolyte volume transfer and vanadium species transport by convection and electro-migration are not considered. To the best of our knowledge, the capacity loss by vanadium species crossover with the electrolyte transfer mechanism has not been investigated in the literature. As reviewed in [35], the crossover of vanadium species by diffusion of ions and electrolyte transfer are the two most significant factors that account for the loss of VRFB capacity over long operational cycles. Therefore, an investigation of the capacity loss caused by the crossover of vanadium species, which considers the mechanism of electrolyte transfer, is necessary in this context. It should be noted that both convection and electro-migration may have non-negligible influences on the crossover of vanadium species.

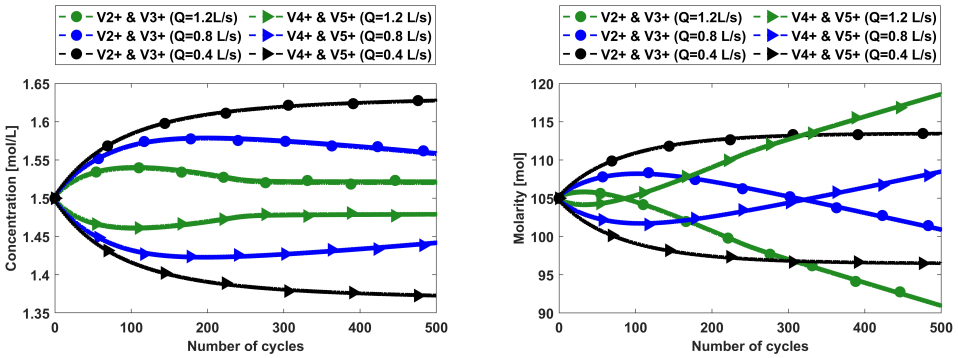

(a) Concentration of positive and negative electrolyte

(b) Molarity of positive and negative electrolyte

Figure 6: The concentration and molarity profiles of vanadium ions in the negative and positive electrolytes with flow rates of 0.4, 0.8, 1.2 L/s and current of 100A during 500 cycles

A simulation study is carried out using charge and discharge currents of 100 A and constant flow rates of 0.4, 0.8, and 1.2 L/s for 500 cycles. From Fig. 6 (a), it can be seen that the electrolyte imbalance initially increased and then decreased to a lower level with a flow rate of 0.8 and 1.2 L/s. At a low flow rate of 0.4 L/s, the electrolyte concentration imbalance becomes more significant and remains steady after 300 cycles. Furthermore, a higher imbalance level leads to more capacity loss, and capacity can be restored with a decrease in the concentration imbalance level according to the results shown in Fig. 6 (a) and Fig. 4 (a) with a flow rate of 0.8 and 1.2 L/s, respectively. In addition, the results in Fig. 6 (a) indicate that a higher flow rate contributes to reducing the electrolyte imbalance and reaching steady state earlier. With movement of the electrolyte from the negative to the positive side, it increases the concentration difference between these two sides and thus facilitates the diffusion of V_2^+ and V_3^+. The Nafion 115 membrane has a higher diffusion capacity for vanadium species in the positive electrolyte than in the negative electrolyte. This leads to a net transfer of vanadium species from the positive to the negative side during a full charge and discharge cycle, as reported in [8]. When the electrolyte volume transfer mechanism is taken into account, it reduces the disparity in diffusion capability between the negative and positive electrolytes. An increase in the electrolyte flow rate causes a more rapid

electrolyte transfer, thus expanding the concentration difference between the negative and positive electrolytes. It accelerates the crossover of vanadium species from the high-concentration (negative) side to the low-concentration (positive), thus further reducing the disparity in diffusion capability between the negative and positive electrolytes and the overall crossover rate from the positive electrolyte to the negative electrolyte. The experimental validation by Nourani et al. [36] and other model-based studies by Tang et al. [8] and Chen et al. [37] proved that the change of the crossover rate influences the long-term capacity retention outcomes. It is evident that higher crossover rates cause more imbalanced electrolyte concentrations and more rapid capacity fading [8, 36, 37].

The result in Fig. 6 (b) shows that a higher electrolyte flow rate accelerates the transport of species from negative to positive electrolyte due to the increase in volume transfer. Electrolyte transfer resulting from the lower flow rate of 0.4 L/s has a negligible impact, indicating that diffusion-driven vanadium ion conversion continues to dominate during the 500 cycles. However, with an increase in the number of cycles and the electrolyte volume difference becoming more significant, the transport of the vanadium ion species from the negative electrolyte to the positive electrolyte becomes inevitable. In summary, when electrolyte transfer is considered, different flow rates have a significant impact on the electrolyte imbalance, affecting the diffusion process to some extent. Higher flow rates help reduce electrolyte concentration imbalance and mitigate associated capacity loss in the early stages. However, substantial electrolyte transfer caused by high flow rates results in long-term capacity loss, which can only be restored by electrolyte re-balancing [38].

To investigate the influence of electro-migration, convection, and diffusion on the crossover of vanadium species, the corresponding fluxes of V^{3+} and V^{4+} are given in Fig. 7 (a) and (b). Note that the direction of flux and charge/discharge period are distinguished in both figures using arrows and a red dashed line. From both figures, it can be seen that the crossover fluxes by electro-migration and convection are bi-directional, where both are mainly driven by the electric field in the electrolyte. The diffusion flux is a uni-directional transport that is mainly driven by the chemical potential gradient of the vanadium species (concentration) across the membrane. The values of the fluxes in the membrane by the three mechanisms at three different positions are shown using the simulation results of a 2-D transient model in [23]. Their simulation results show that the vanadium ion crossover driven by the electric field is minor compared with diffusion, and their net transport directions are different during the charging and discharging processes. Most importantly, species transport by electro-migration and convection has an impact on the crossover of vanadium ions, as indicated in Fig. 7 (a) and (b). Nevertheless, its impact is limited where the major flux through the membrane is still by diffusion.

A different simulation study is conducted to further analyse different crossover mechanisms on the capacity loss of VRFB systems for the 5 kW/3 kWh VRFB system. In this study, the operational current and the electrolyte flow rate are the same as in the previous case study. The molarity and concentration of the negative electrolyte and the capacity changes over time with the different mechanisms involved are shown in Figs. 7 (c), (d), and (e). In Fig. 7 (c), it is clear that transport of the negative electrolyte to the positive electrolyte takes place regardless of whether electro-migration and convection are involved or not. This shows that the crossover of vanadium species is mostly driven by diffusion and osmosis strengths, as explained previously. However, the results in Fig. 7 (d) indicate that the electrolyte concentration imbalance is different with the consideration of different mechanisms. This is because the net transport directions by electro-migration and convection are different, which could decrease/strengthen the transport of V^{2+} and V^{3+}. Furthermore, the results in Figs. 7 (a) and (b) provide evidence that electro-migration has

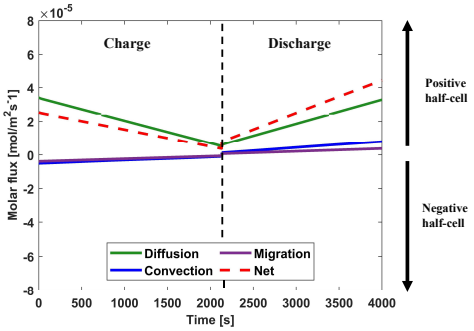

(a) Diffusion, convection electro-migration, and net fluxes of V_3^+ inside a single cell

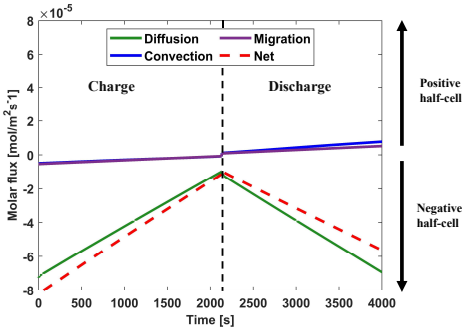

(b) Diffusion, convection electro-migration and net fluxes of V_4^+ inside a single cell

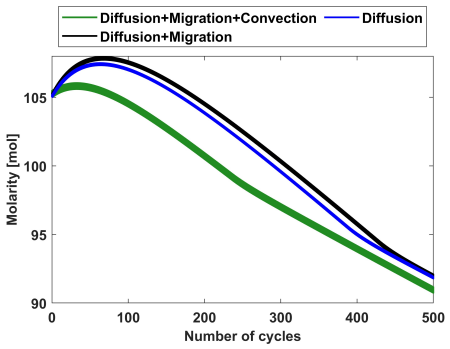

(c) Molarity of negative electrolyte with different crossover mechanisms involved over 500 cycles

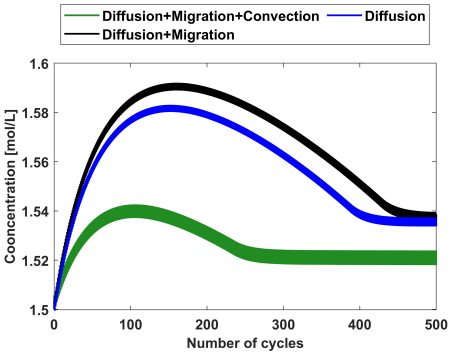

(d) Concentration of negative electrolyte with different crossover mechanisms involved over 500 cycles

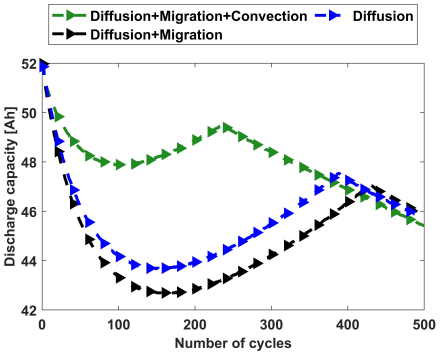

(e) Capacity profiles with different crossover mechanisms involved over 500 cycles

Figure 7: The flux profiles of one complete charge/discharge cycle and the molarity, concentration, and capacity profiles over 500 cycles considering combinations of the different crossover mechanisms for this 5 kW/3 kWh VRFB system

the lowest impact on the electrolyte imbalance compared to convection and diffusion. The capacity profiles shown in Fig. 7 (e) indicate that the capacity changes differently to some extent before 400 cycles, which is due to different crossover mechanisms that influence the level of electrolyte concentration imbalance. As mentioned by Yang et al. in [23], the vanadium-ion crossover under the influence of the electric field still plays a significant role in capacity loss, which cannot be ignored in long-term battery operation.In previous research studies, the role of the electric field in the crossover was not adequately investigated because there were no long-term model-based studies or in-depth analyses. 0-D VRFB transient models that only consider the diffusion effect may lead to inaccurate simulation results. Hence, it is crucial to pay attention to the influence of the electric field in vanadium ion crossover and capacity loss for a more comprehensive understanding and accurate predictions. Fig. 7 (d) shows that after 400 cycles, as the electrolyte concentration imbalance becomes stable, the loss of capacity becomes proportional to the number of cycles due to the ongoing transfer of the electrolyte volume by osmosis. Therefore, electrolyte concentration imbalance is the main underlying factor that causes capacity loss at an early stage, and electrolyte volume transfer by osmosis becomes more significant with increasing number of cycles. In conclusion, the two most influential factors in capacity loss are electrolyte volume transfer and diffusion, which act in tandem. Moreover, from the results so far, it can be concluded that a higher electrolyte flow rate tends to reduce the electrolyte concentration imbalance for capacity loss reduction. However, it will cause long-term capacity loss by electrolyte volume transfer, which will be more significant. The influence of the electric field is not that significant due to the relatively low electro-kinetic permeability of the Nafion 115 membrane over many operational cycles.

Another critical aspect to consider is the significant variation in the effects of different crossover mechanisms in different VRFB systems. For instance, in the single cell VRFB system mentioned earlier, the impact of convection flux is limited because of the small electrolyte flow rate and electrode area, while electro-migration under the influence of an electric field becomes more dominant. Consequently, varying charging/discharging times and higher electric fields can lead to increased transfer of vanadium species from the positive half-cell to the negative half-cell, exacerbating concentration imbalances and resulting in more substantial capacity losses. Yang et al. highlighted that the effect of the electric field on the crossover of vanadium ions has a considerable long-term impact on discharge capacity performance from the results in [23]. This underscores the critical need for accurate modelling tailored to different VRFB systems to achieve accurate SOH estimation and capacity loss analysis. The model proposed in this study can effectively achieve these objectives, and its low computational complexity facilitates seamless implementation in hardware systems with limited computational resources.

3.4. The capacity loss from electrolyte flow rate and operational current

Karrech et al. drew an important conclusion in [16] that the electrolyte flow rate influences the discharge capacity of a VRFB system, which is also known as DOD. The reason behind this is that a higher electrolyte flow rate will reduce the concentration overpotentials, thus increasing the time required to reach the charging and discharging cut-off voltage limits. Furthermore, the operational current is another factor that determines the DOD level under the same electrolyte flow rate. This is caused by the fact that a higher current produces higher overpotentials, which means that battery charging or discharging ends earlier due to the cutoff limits. Generally, a higher electrolyte flow rate or lower operational current will increase discharge capacity.

To investigate the effect of electrolyte flow rate and current on the final SOC during the charging and discharging level of the 5 kW/3 kWh VRFB system, simulations were performed

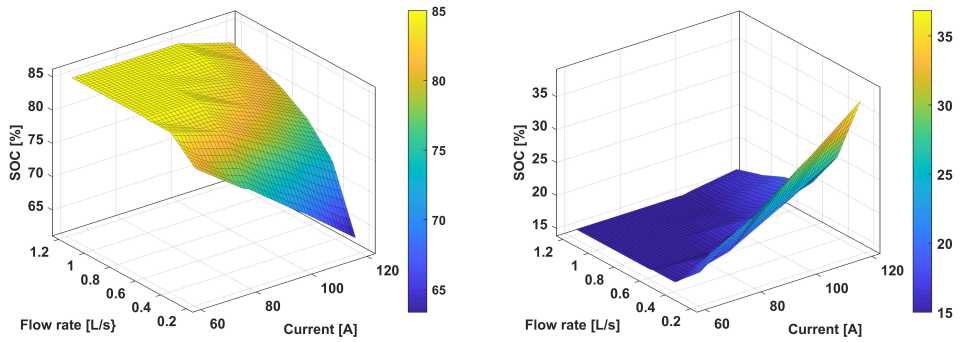

(a) The final SOC after being charged under different flow rates and currents

(b) The final SOC after being discharged under different flow rates and currents

Figure 8: The final SOC level being charged and discharged under different flow rates and currents of this 5 kW/3 kWh VRFB system

and the results are presented on two 3D surfaces as shown in Fig. 8. Here, it is assumed that this VRFB system was initially balanced with a SOC of 15% and then charged and discharged to the cutoff voltage limits. It can be seen from both figures that higher currents and/or lower flow rates prevent the VRFB system from being charged or discharged to a higher level and vice versa. In Fig. 4 (a), the low capacity obtained with a flow rate of 0.4 L/s and 0.2 L/s is caused by this reason. In most real-world applications using VRFB for energy storage, constant current-constant voltage (CC-CV) and other charging current limiting regimes can be used to achieve higher SOC levels when the VRFB is being charged. However, in an energy system, normally the discharge current cannot be limited due to the customers' demand. The product specification for UPOWER by Rongke Power has shown that their VRFB system has a rated capacity of 40 kWh under 10 kW discharge power [39]. However, at a 14 kW discharge power level, the discharge capacity is only 28 kWh. The loss of discharge capacity is inevitable in high-power discharge applications, and a decrease in discharge power can extend the discharge capacity. Moreover, a higher electrolyte flow rate of pumps is critical to obtaining high VRFB system discharge capacities in high-power applications. The research studies presented by Tang et al. [15], Karrech et al. [16] and Wang et al. [31] highlight the need to use a variable flow rate to reduce capacity loss and pump power consumption. Nevertheless, the technical and economic feasibility of this idea in an industrial VRFB device needs further investigation.

4. Conclusion

In this paper, a new 0-D dynamic VRFB model is developed considering both the electrolyte transfer and the vanadium species crossover mechanisms. The proposed model is validated using the experimental data from a 5 kW/3 kWh VRFB system under three different constant current regimes and from a single cell VRFB system, tested by PNNL. The proposed model shows good performance in voltage and capacity estimation in agreement with the experimental data. Based on the proposed model, the capacity loss mechanisms for the 5 kW/3 kWh VRFB system are comprehensively analysed. The loss of capacity caused by the electrolyte volume transfer as a

result of osmosis is found to be the most significant factor that leads to the long-term loss of capacity for VRFBs. In addition, crossover by diffusion is the main cause of electrolyte imbalance that leads to capacity loss. The simulation results show that the electrolyte transfer mechanism escalates the crossover due to ion diffusion to some extent. Nevertheless, the ion crossover driven by the electric field and velocity inside the membrane cannot be ignored. Otherwise, it will lead to poor long-term capacity estimation results. Finally, the influence of the electrolyte flow rate and operational current on the VRFB charge and discharge level is highlighted, which offers practical insight into the reduction of capacity loss in high-power scenarios. The proposed model is well suited to be used by control and optimisation algorithms in different applications. It is also useful for model-based studies related to the development of electrolyte rebalancing techniques and the estimation of SOH. However, it is still notable that because of the technical restrictions, the inaccuracy of membrane and electrode parameters can severely limit the accuracy of SOH and battery state estimation. For future work, it is important to validate the feasibility and precision of the proposed 0-D model in the estimation of SOH for a wider range of industrial-scale VRFB systems with accurately measured parameters.

Acknowledgment

This project is supported by the Australian Government Research Training Program (RTP) through the University of Adelaide, and a supplementary scholarship is provided by the Microgrid Battery Deployment project, which is funded by the Future Battery Industries Cooperative Research Centre (FBICRC) as part of the Commonwealth Cooperative Research Centre Program, Australia.

Declaration of Generative AI and AI-assisted technologies in the writing process

During the preparation of this work, the authors used Writefull/Grammarly for grammar checking. After using these tools, the authors reviewed and edited the content as needed and take full responsibility for the content of the publication.

CRediT authorship contribution statement

Hao Wang: Conceptualization, Investigation, Methodology, Software, Validation, Formal analysis, Writing – original draft, Writing – review & editing, Visualization. **S. Ali Pourmousavi**: Conceptualization, Writing – review & editing, Supervision, Project administration. **Yifeng Li**: Conceptualization, Methodology,Writing – review & editing, **Wen L. Soong**: Conceptualization, Writing – review & editing, Supervision. **Xinan Zhang**: Writing – review & editing, Supervision. **Bingyu Xiong**: Data curation.

References

[1] Hao Wang, S Ali Pourmousavi, Wen L Soong, Xinan Zhang, and Nesimi Ertugrul. Battery and energy management system for vanadium redox flow battery: A critical review and recommendations. *Journal of Energy Storage*, 58:106384, 2023.

[2] Katharina Schafner, Maik Becker, and Thomas Turek. Capacity balancing for vanadium redox flow batteries through continuous and dynamic electrolyte overflow. *Journal of Applied Electrochemistry*, 51(8):1217–1228, 2021.

[3] AA Shah, MJ Watt-Smith, and FC Walsh. A dynamic performance model for redox-flow batteries involving soluble species. *Electrochimica Acta*, 53(27):8087–8100, 2008.

[4] Ertan Agar, KW Knehr, D Chen, MA Hickner, and EC Kumbur. Species transport mechanisms governing capacity loss in vanadium flow batteries: Comparing nafion® and sulfonated radel membranes. *Electrochimica acta*, 98:66–74, 2013.

[5] KW Knehr, Ertan Agar, CR Dennison, AR Kalidindi, and EC Kumbur. A transient vanadium flow battery model incorporating vanadium crossover and water transport through the membrane. *Journal of The Electrochemical Society*, 159(9):A1446, 2012.

[6] Qiong Zheng, Huamin Zhang, Feng Xing, Xiangkun Ma, Xianfeng Li, and Guiling Ning. A three-dimensional model for thermal analysis in a vanadium flow battery. *Applied energy*, 113:1675–1685, 2014.

[7] Kyeongmin Oh, Milad Moazzam, Geonhui Gwak, and Hyunchul Ju. Water crossover phenomena in all-vanadium redox flow batteries. *Electrochimica Acta*, 297:101–111, 2019.

[8] Ao Tang, Jie Bao, and Maria Skyllas-Kazacos. Dynamic modelling of the effects of ion diffusion and side reactions on the capacity loss for vanadium redox flow battery. *Journal of Power Sources*, 196(24):10737–10747, 2011.

[9] Ao Tang, Jie Bao, and Maria Skyllas-Kazacos. Thermal modelling of battery configuration and self-discharge reactions in vanadium redox flow battery. *Journal of Power Sources*, 216:489–501, 2012.

[10] Rajagopalan Badrinarayanan, Jiyun Zhao, KJ Tseng, and Maria Skyllas-Kazacos. Extended dynamic model for ion diffusion in all-vanadium redox flow battery including the effects of temperature and bulk electrolyte transfer. *Journal of Power Sources*, 270:576–586, 2014.

[11] Yifeng Li, Maria Skyllas-Kazacos, and Jie Bao. A dynamic plug flow reactor model for a vanadium redox flow battery cell. *Journal of Power Sources*, 311:57–67, 2016.

[12] M Pugach, M Kondratenko, S Briola, and A Bischi. Zero dimensional dynamic model of vanadium redox flow battery cell incorporating all modes of vanadium ions crossover. *Applied energy*, 226:560–569, 2018.

[13] Yuxi Song, Xiangrong Li, Jing Xiong, Linlin Yang, Guoliang Pan, Chuanwei Yan, and Ao Tang. Electrolyte transfer mechanism and optimization strategy for vanadium flow batteries adopting a nafion membrane. *Journal of Power Sources*, 449:227503, 2020.

[14] Kyeongmin Oh, Seongyeon Won, and Hyunchul Ju. A comparative study of species migration and diffusion mechanisms in all-vanadium redox flow batteries. *Electrochimica Acta*, 181:238–247, 2015.

[15] Ao Tang, Jie Bao, and Maria Skyllas-Kazacos. Studies on pressure losses and flow rate optimization in vanadium redox flow battery. *Journal of power sources*, 248:154–162, 2014.

[16] A Karrech, K Regenauer-Lieb, and F Abbassi. Vanadium flow batteries at variable flow rates. *Journal of Energy Storage*, 45:103623, 2022.

[17] Seong Beom Lee, Kishalay Mitra, Harry D Pratt III, Travis M Anderson, Venkatasailanathan Ramadesigan, Babu R Chalamala, and Venkat R Subramanian. Open data, models, and codes for vanadium redox batch cell systems: a systems approach using zero-dimensional models. *Journal of Electrochemical Energy Conversion and Storage*, 17(1):011008, 2020.

[18] Yifeng Li. *Advanced Modelling, Optimisation and Control of Vanadium Redox Flow Battery*. PhD thesis, The University of New South Wales, 2018.

[19] Yifeng Li, Longgang Sun, Liuyue Cao, Jie Bao, and Maria Skyllas-Kazacos. Dynamic model based membrane permeability estimation for online soc imbalances monitoring of vanadium redox flow batteries. *Journal of Energy Storage*, 39:102688, 2021.

[20] Ankur Bhattacharjee and Hiranmay Saha. Development of an efficient thermal management system for vanadium redox flow battery under different charge-discharge conditions. *Applied Energy*, 230:1182–1192, 2018.

[21] Bahman Khaki and Pritam Das. Voltage loss and capacity fade reduction in vanadium redox battery by electrolyte flow control. *Electrochimica Acta*, 405:139842, 2022.

[22] Lorenz Gubler. Membranes and separators for redox flow batteries. *Current Opinion in Electrochemistry*, 18:31–36, 2019.

[23] Xiao-Guang Yang, Qiang Ye, Ping Cheng, and Tim S Zhao. Effects of the electric field on ion crossover in vanadium redox flow batteries. *Applied energy*, 145:306–319, 2015.

[24] Yuan Lei, BW Zhang, BF Bai, and Tim S Zhao. A transient electrochemical model incorporating the donnan effect for all-vanadium redox flow batteries. *Journal of Power Sources*, 299:202–211, 2015.

[25] Jeongmin Shin, Chanyoung Kim, Byeongseon Jeong, Neil Vaz, and Hyunchul Ju. New operating strategy for all-vanadium redox flow batteries to mitigate electrolyte imbalance. *Journal of Power Sources*, 526:231144, 2022.

[26] Ertan Agar, A Benjamin, CR Dennison, D Chen, MA Hickner, and EC Kumbur. Reducing capacity fade in vanadium redox flow batteries by altering charging and discharging currents. *Journal of Power Sources*, 246:767–774, 2014.

[27] Philipp A Boettcher, Ertan Agar, CR Dennison, and E Caglan Kumbur. Modeling of ion crossover in vanadium redox flow batteries: a computationally-efficient lumped parameter approach for extended cycling. *Journal of The Electrochemical Society*, 163(1):A5244, 2015.

[28] Jovan Kamcev, Rahul Sujanani, Eui-Soung Jang, Ni Yan, Neil Moe, Donald R Paul, and Benny D Freeman. Salt concentration dependence of ionic conductivity in ion exchange membranes. *Journal of Membrane Science*, 547:123–133, 2018.

[29] Yasser Ashraf Gandomi, DS Aaron, TA Zawodzinski, and MM Mench. In situ potential distribution measurement and validated model for all-vanadium redox flow battery. *Journal of The Electrochemical Society*, 163(1):A5188, 2015.

[30] Christian Lutz, Sven Hampel, Xi Ke, Sabine Beuermann, Thomas Turek, Ulrich Kunz, Ana Guilherme Buzanich, Martin Radtke, and Ursula EA Fittschen. Evidence for redox reactions during vanadium crossover inside the nanoscopic water-body of nafion 117 using x-ray absorption near edge structure spectroscopy. *Journal of Power Sources*, 483:229176, 2021.

[31] Hao Wang, S Ali Pourmousavi, Wen L Soong, Xinan Zhang, Nesimi Ertugrul, and Bingyu Xiong. Model-based nonlinear dynamic optimisation for the optimal flow rate of vanadium redox flow batteries. *Journal of Energy Storage*, 68:107741, 2023.

[32] S König, MR Suriyah, and T Leibfried. Innovative model-based flow rate optimization for vanadium redox flow batteries. *Journal of Power Sources*, 333:134–144, 2016.

[33] Yun Wang and Sung Chan Cho. Analysis and three-dimensional modeling of vanadium flow batteries. *Journal of The Electrochemical Society*, 161(9):A1200, 2014.

[34] PNNL open datasheets for test VRFB systems, Mar 2021. `https://data.pnnl.gov/group/nodes/dataset/13497`.

[35] Tossaporn Jirabovornwisut and Amornchai Arpornwichanop. A review on the electrolyte imbalance in vanadium redox flow batteries. *International Journal of Hydrogen Energy*, 44(45):24485–24509, 2019.

[36] Mahnaz Nourani, Christopher R Dennison, Xinfang Jin, Fuqiang Liu, and Ertan Agar. Elucidating effects of faradaic imbalance on vanadium redox flow battery performance: Experimental characterization. *Journal of The Electrochemical Society*, 166(15):A3844, 2019.

[37] Yunxiang Chen, Jie Bao, Zhijie Xu, Peiyuan Gao, Litao Yan, Soowhan Kim, and Wei Wang. A hybrid analytical and numerical model for cross-over and performance decay in a unit cell vanadium redox flow battery. *Journal of Power Sources*, 578:233210, 2023.

[38] Arjun Bhattarai, Nyunt Wai, Rüdiger Schweiss, Adam Whitehead, Günther G Scherer, Purna C Ghimire, Tuti M Lim, and Huey Hoon Hng. Vanadium redox flow battery with slotted porous electrodes and automatic rebalancing demonstrated on a 1 kw system level. *Applied Energy*, 236:437–443, 2019.

[39] UPOWER series (Rongke power), June 2023. `http://www.rongkepower.com`.